Variation in hydrologic connectivity as a result of microtopography explained by discharge to catchment size relationship

M.R.Oosterwoud [1,2], M.J. van der Ploeg [1], S. van der Schaaf [1] and S.E.A.T.M. van der Zee [1]

Soil Physics and Land Management Group, Wageningen University, The Netherlands
Department Hydrogeology, Helmholtz Centre for Environmental Research, Leipzig, Germany
School of Chemistry, Monash University, Victoria, Australia

Abstract

In hydrological terms raised bogs can be approximated by simple models as in the acrotelm-catotelm concept. However, raised bogs are often characterized by a pronounced surface topography, causing large changes in connectivity of contributing areas onthe bog. In this study, daily regression of measured discharges versus catchment areas is used to quantify the importance of surface topography on catchment connectivity within a raised bog. The resulting coefficient of determination shows the strengthof the relationship between the discharge and catchment area over time under different hydrological conditions. Monitoring of discharge, water table, transmissivity, and basic weather data on a raised bog (1.9km ^{2}) in eastern central Estonia took place from May 2008 to June 2010. Contributing areas, calculated based on the outlet's discharge volume (V_Q) divided by the net precipitation volume ($V_{P_{\mathrm{net}}}$), of the outlet containing the central pool-ridge system varied between 1 $mes10^{-3}$ m ^{2} and 0.7km ^{2}, suggesting significant differences in connectivity between hydrological events. Correlation between discharge and theoretical catchment size was high (R^2>0.75) when the water table was closeto the surface (less than 5 cm below peat surface), and consequently transmissivities were also high (up to 1030 m ^{2} d $^{-1}$), which lead to connectivity of local storage elements, such as pools and hollows. However, a water table below this threshold resulted in large parts of the catchment being disconnected. The importance of water table depths on catchment connectivity suggests the need to reconsider the hydrological concept of raised bogs; to incorporate these shallow flow components and better understand residence time and consequently transport of solutes, such as DOC, from patterned peatlands.

This article has been accepted for publication and undergone full peer review but has not been through the copyediting, typesetting, pagination and proofreading process which may lead to differences between this version and the Version of Record. Please cite this article as doi: 10.1002/hyp.11164

Introduction

Peatlands are primarily characterised by their high organic matter content and ability to retain large amounts of water (up to 90% by volume). The integrity of raised bogs is only ascertained when water stored in the peat body is retained during periods of precipitation deficit, yet efficiently removed in wet periods [35,2]. The high water storage capacity of the upper peat layer and its ability to shrink and swell facilitates a relative stable water table close to the bog's surface [16]. The capacity to retain water under drought is enhanced by the strong decrease of hydraulic conductivity as a function of depth as a result of compaction [24] and degree of decomposition [4,34]. The feedback between hydrology and plant species facilitates the distinctive microtopographic structures found on raised bogs, such as hummocks, hollows, lawns and ridges [9]. Large differences in hydraulic properties as well as biogeochemical regimes exist between the different surface pattern features [30,5].

The transition in peat structure, as evident by the change in bulk density and hydraulic conductivity over depth, led to the acrotelm-catotelm concept [17]. The acrotelm serves as the aquifer with little decomposition and a high hydraulic conductivity and storage capacity, whereas the catotelm is more inert, owing to more humified and permanently saturated conditions. In contrast to the original concept of [17], [14] and tetclymo-limits-1984 also considered biological processes, like peat growth and decomposition rates and the transition between oxic and anoxic zones, in the partitioning between the acrotelm and catotelm.

[15] provided the relationship between water table depth and lateral flow for a theoretical raised bog with uniform saturated hydraulic conductivity. Ingram's proposed model was based on the Dupuit-Forchheimer approximation for Darcy's law, in which vertical flow is disregarded and the slope of the water table is equal to the hydraulic gradient:

$$\frac{U}{K} = \frac{H^2}{L^2} \tag{1}$$

where U (md $^{-1}$) is net recharge (precipitation (P) - evapotranspiration (ET)), K (md $^{-1}$) is horizontal hydraulic conductivity, H (m) is head above drainage base, L (m) is the distance from the bog's edge to the bog's hydrological divide.

Since hydraulic conductivity varies strongly with depth, it is considered more appropriate to use transmissivity in flow calculations [31]. Transmissivity is the product of hydraulic conductivity and layer thickness of each layer contributing to flow. Based on Ingram's assumptions this would imply that a falling water table results in a

1. *reduced hydraulic gradient between the bog's dome and its margin and*
2. *a lower transmissivity due to reduced thickness of flow*

.

However, in contrast to Ingram's assumptions, peat properties such as hydraulic conductivity, porosity and water retention parameters are seldom constant with depth. Due to the water table depth variable transmissivity, a change in water table depthalso affects lateral flow.

Patterned raised bogs consist of ridge-pool or ridge-hollow topography. Ridges are oriented perpendicular to the main flow direction, but may have low-lying preferential flow paths that increase connectivity between adjacent pools during periods of high water table [25]. These preferential flow paths, generally occurring as superficial shallow channels affect the lateral flow of water. For low-angle terrain, [8] and [1] showed that as soon as the global gradient of elevation is sufficiently smaller than the size of local microtopographical variations a fill-and-spill process becomes important. This fill-and-spill process adds complexity to the flow patterns [33], as ponded depressions may merge during wetting, or separate during drying. The role of soil surface flow in wetlands was addressed by [22], who showed the formation of complex patterns of water ponding and redistribution when microtopographical variation was considered (see Fig. 1).

The acrotelm-catotelm concept is deeply ingrained into current thinking about peatland hydrological processes and structures. However, both theoretical [3,20] and experimental [12] studies have identified a number of limitations to the acrotelm-catotelm model and have advocated the need for the peatland community to adopt more flexible cohort based models of peatland development [21]. Beside the limitations in describing peatland development over longer periods, the acrotelm-catotelm concept's simplicity is possibly also a limitation for describing the dynamics of patterned bog hydrology over shorter periods. The assumptions of a homogeneous bog, with idealised geometry and boundary conditions, ignores the reality of a strong spatial variable surface topography and peat structure.
In this paper, we specifically elaborate on the discharge of a raised bog by analysing experimental data including discharge, groundwater levels and transmissivity from a raised bog in Estonia. We tested measured data against common approaches from citetingram-size-1982 and [17] to describe the flow of water on a raised bog.
We hypothesise that

1. *preferential flow paths in the pool-ridge complex play a crucial role in temporal variation in*
2. *flow direction and*
3. *the internal distribution of water on the bog* .

Material and methods

Site description

In eastern central Estonia, south of the Pandivere Upland, poorly drained depressions as a result of bedrock topography and glacial deposits have led to the formation of lakes and bogs. The raised bogs in this area formed ca. 3500 years ago on top of fen peat that developed 8000 years ago on lake deposits in the eastern part of the post-glacial lake Suur-Endla [13,27]. Männikjärve bog is a convex raised bog located in central Estonia (N 58 52 °, E 26 15 °) and is part of the larger Endla nature reserve. The bog's surface topography is characterized by areas of different surface topographical features, with a central pool-ridge complexes and pine bog forest at the margin. Hummocks and hollows range in size from a few decimeters to several meters. Differences in surface level between hummocks and hollows are mostly less than 40 cm, although locally higher hummocks occur. The total area of the bog is $\sim 1.9 km^2$, and the peat in the central part of the bog reaches a thickness of $\sim$ 7m [13]. The pools within the pool-ridge complex have and elongated shape with an average depth of 1 m and 1.5m (maximum of 2.5m) [18] and cover $\sim$ 3% of the total surface. From an aerial photograph 103 pools have been identified, the surface area of the pools ranges from 20m ^{2} and 8639m ^{2} and their perimeter ranges from 18 m and 1477m. The bog's surface has a relatively flat slope oriented from east to west, with a gradient of $\sim$ 0.2% from the central part of the bog until the pool-ridgecomplex. Towards the western margin, the bog has a slope with a gradient of $\sim$ 0.5%. Typical plant species found on ridges and hummocks of Männikjärve bog are *Sphagnum fuscum*, *Calluna vulgaris*, *Ledum palustre*, and *Andromeda polifolia*. In hollows and lawns the vegetation is dominated by *Sphagnum cuspidatum*, *Scheuchzeria palustris*, and *Carex* sp. Towards the margins the contribution of *Pinus sylvestris* increases.
In 1910 an experimental mire station was established in Tooma village close to Männikjärve bog in order to perform studies related to the drainage of bogs; old drainage ditches are still visible on the eastern margin of the bog. Since 1950 a hydro-meteorological station has been operated on Tooma mire station by the Estonian Meteorological and Hydrological Institute (EMHI). In 1963 the bog was surrounded by marginal ditches to prevent it from expanding laterally [13].

Data acquisition

Hydrological monitoring took place from May 2008 to June 2010. The Estonian Meteorological and Hydrological Institute (EMHI) provided daily values for discharge from three V-notch weirs (Q1, Q5, Q7, shown in Fig. 2), precipitation and snow depth, evaporation from pools (GGI 3000 pan, USSR), evapotranspiration (GGI-B-1000 evaporimeter, USSR), and air temperature from their field station. Two additional V-notch weirs (Q2 and Q3) were installed to capture discharge at the north boundary of the bog. Additionally, Männikjärve bog was instrumented for measurements of water table along an east-west transect (Fig. 2). Precipitation was measured continuously with a tipping bucket rain gauge (Lambrecht) located in the pool-ridge complex. Piezometers were installed at nine locations along an approximately 1km E-W transect across the bog to capture the main microtopographic zones, including the pool-ridge zone. The piezometers were constructed from PVC tubes with a diameter of 4.5 cm, which were perforated over 50 cm starting 10 cm below the bog's surface. Each piezometer was equipped with a pressure transducer (Diver, Schlumberger) that recorded at 30 min intervals. A separate pressure transducer (Diver) recorded the atmospheric pressure. In preparation of the hydrological monitoring that happened from 2008–2010, transmissivity was measured at 26 locations (see Fig. 2) eight times under different water table conditions during 2002 to 2004 using the semi-steady state method followed by the pit-bailing method [32].

Data analysis

Discharge and water table time-series analysis

Data from pressure transducers (bog, pool, and upstream of two V-notch weirs) was corrected for atmospheric pressure. Twice yearly the measured pressure heads were adjusted to manually measured water levels. Discharge at Q2 and Q3 was determined from rating curves and upstream water levels. Discharge, water level, and precipitation records were aggregated into daily values using R [26]. To eliminate disturbances in the measured water levels and discharges caused by frost and snow, the hydrological year was restricted to frost free periods (mean daily temperature above zero). The amount of water coming from the remaining snow cover at the start of the frost free period was estimated from snow depth and snow density data.

Transmissivity

The 26 locations at which transmissivity was measured were grouped by ecotope based on their location on the bog. For each ecotope, the measured transmissivities and their water tables were fitted to Eq. 2 using a non-linear least squarefunction (R package nls2, [11]).

$$T = \frac{K_{max \times (1-h)^{1-M}}}{M-1} \tag{2}$$

where T is transmissivity in m $^2 d^{-1}$, h is water table depth in m, $K_{\max}$ is maximal saturated hydraulic conductivity at the peat surface in md $^{-1}$ and M is parameter describing the rate of decrease in hydraulic conductivity with depth.

To estimate the starting values the brute-force algorithm was used followed by a non-linear least square (nls) optimization to obtain values for $K_{\max}$ and M. Since water table is considerably easier to monitor compared to measuring tranmissivity, once values for $K_{\max}$ and M are obtained water table data can be used to estimate transmissivity values for a similar location using Eq. 2.

Topographic catchment area and correlation with discharge

To assess the daily variation in the relationship between discharge and its catchment area the daily discharge time series were used. Based on contour lines and point measurements obtained from a topographical map (scale 1:10000) a flownet was created (QGIS GRASS: r.flow), which defined the general direction of lateral flow in the bog. This flownet was used to obtain the internal catchment boundaries of the four outlets (Q) (Fig. 2). Catchment size for each outlet was calculated from the digitised polygon features obtained from the watershed delineation routine (QGIS GRASS: r.watershed). With the use of the derived catchment areas, a daily regression of the discharge at the four outlets (Q, Ls $^{-1}$) versus theircatchment areas (A, m ^{2}) was computed [29]. The resulting daily coefficient of determination (R^2) shows the strength of the proportion between the discharge and catchment area over time under different hydrological conditions. A change in the proportion between the discharges results in an unbalance between the catchment size and amount of discharge and, therefore, a reduced R^2 value.

Event dependent contributing area

To estimate the size of the contributing area for each outlet under different hydrological conditions, we selected hydrological events based on the 90th percentile precipitation events (> 12 mm d $^{-1}$) (see Table A.1). This resulted in a total of eighteen events (see Appendix B and Fig. C.1). For each event the size of the contributing areas was calculated based on the outlet's discharge volume (V_Q) over the duration of theevent divided by the net precipitation volume ($V_{P_{\text{net}}}$) over the same period:

$$A = \frac{V_Q}{V_{P_{\text{net}}}} \quad (3)$$

where A is the catchment's contributing area (m ^{2}), V_Q is the discharge volume (m ^{3}) and $V_{P_{\text{net}}}$ is net precipitation volume (m). The resulting sizes of the contributing areas can be compared with the theoretical catchment areas based on the bog's surface gradient.

Statistical analysis

We used a Kruskal-Wallis test to determine if water table behaviour at different locations/piezometers (i.e. microforms) is significantly different. The Kruskal-Wallis test allows for testing differences between two or more groups that are not necessarilynormally distributed. A post-hoc Dunn test allowed for the identification of individual locations/piezometers that are significantly different.

Results

Water balance

Total precipitation during the study period was largest in 2008 with 638 mm, followed by 2009 and 2010 with 520 mm and 422 mm, respectively (Table 1). Unlike 2010, when precipitation was fairly evenly distributed over the year and snowmelt had a large contribution to the total precipitation input, a substantial proportion of the 2008 and 2009 precipitation occurred in the summer months. Water losses caused by evapotranspiration were larger than the losses by discharge(see Table 1). During the summer months evapotranspiration was often equal to or slightly larger than the precipitation inputs. Storage changes had a pronounced seasonal pattern, with decreasing storage during the summer months and recharge during the spring and autumn periods. Whilst 2008 had the largest precipitation amounts, the net storage deficit is smallest in 2009.

Discharge

A clear discharge peak marks the snowmelt in 2009 and 2010 as soon as the air temperature rises above zero (Fig. 3). After the snowmelt period, discharges reduce as a result of increasing evapotranspiration losses. The average daily discharge from the entire bog was ~ 3 Ls $^{-1}$. The large discharge peak at outlet Q3 observed during the period before the snowmelt in 2010 is questionable, since temperatures were still well below zero. Spatial differences in snowpack distribution could have resulted in differences in snowmelt water inputs towards the different outlets. However, this is unlikely to have played a role here as EMHI measurements found good agreement between snow depths measured at three locations (data not shown). Furthermore, even though the frost period was over, artifacts due to frozen loggers in our monitoring wells and weirs might have occurred. By disregarding periods when frost occurred, we tried to minimise any artifacts caused by frost.

For the different outlets, three flow situations were defined based on discharge percentiles (see Table A.1): low flow (<25th *P*), normal flow (>25th *P* – <75th *P*), and high flow (>75th *P*). Over the study period there were 487 to 689 days with flow (discharge >0 Ls $^{-1}$) that discharged a total of 2.2 $\times 10^5$ to 3.6 $\times 10^5$ m ^{3} (see Table A.2). The high flow period accounted for 25% of the days, but contributed 70 to 90% of the discharge. Low flow periods represented only 1 to 3% of the total flow. During dry periods, discharge at outlets Q5 and Q7 quickly reduced to almost zero. However, no flow days were far less frequent at outlet Q2 and Q3. Rapid increases in discharge after precipitation events were still observed during the summer months, despite overall lower discharge rates.

Water table

The temporal variability in water table depth of the piezometers showed a similar responds to precipitation input (Fig. 4). For most of the study period the water table was located slightly below the bog surface. In the summer months water tables decreased and extended periods of low water tables were observed during June 2008 and July–September 2010. The position of the water table reflects the outcome of the storage balance ($P-(Q+ET)$), were P and ET are the main water balance terms (Table 1). A positive storage balance results in higher water tables, a negative storage balance results in decreasing water tables.

Although similar trends over time are observed, a water table frequency distribution (Fig. 5) shows that the different piezometer locations have different water table regimes. The results from the Kruskal-Wallis test showed that the differences between the water table regimes measured at the piezometers are significant (Chi-square: 3182 >theoretical 15.5, p-value: <2.2 $\times 10^{-16}$). From the post-hoc Dunn test it can be concluded that all piezometers except W36 and W2 as well as W36 and W27 are significantly different from each other (see Table D.3). Furthermore, also W38 and W5 are not significantly different from each other. Piezometers W36 and W27 are both located in themargin (see Fig. 2). Piezometer W2 is located on the edge of margin to ridge-hollow, however, its water table regime clearly resembles that of the other margin piezometers. Piezometers W38 and W5 are both located on the highest(central) part of the bog.

Transmissivity

Transmissivity was similar across the different topographic zones: with median transmissivities of 15 m ^{2}d $^{-1}$, 17 m ^{2}d $^{-1}$, 17 m ^{2}d $^{-1}$ and 22m ^{2}d $^{-1}$ in order of appearance in Fig. 6. The lower quartile of values were measured during periods of lower water table depths. The greatest transmissivity values occurred during periods of high water tables, facilitating shallow subsurface flow conditions.

For each ecotope, the measured transmissivities and their water tables were fitted to Eq. 2 to obtain values for maximum hydraulic conductivity at the peat surface ($K_{\max}$) and the rate of hydraulic conductivity decrease withdepth (M) (Fig. 7). The largest $K_{\max}$ values occurred at the peat surface of the pool-ridge zone, but decreased fastest with depth. Maximum transmissivities for water tables at the bogs surface ranged from nge351030, respectively in the hollow-ridge and pool-ridge ecotope zones.

Topographic catchment area and correlation with discharge

As the bog's water table is located close to the peat surface, with water draining laterally by gravity [17], the bog's surface gradient is assumed to represent the hydraulic gradient (Fig. 8a). Under these assumptions the bog's surface gradient contains information about the internal catchment boundaries. The two largest sub-catchment areas are those that discharge through Q7 and Q5. They comprised 0.39 km ^{2} and 0.35km ^{2}, respectively, and cover the southern and northern part of the pool-ridge zone (see Fig. 8b). The topography of thesesub-catchments is characterized by a flat surface slope with large hollows at the water divide. Halfway down the slope, the surface slope becomes slightly steeper and the topography becomes more pronounced (pool-ridge zone) (Fig. 8c). Towards the outlets, the topography changes again to hollow-ridge and passes into a narrow margin with bog forest. The two northern sub-catchments, Q2 and Q3, were 0.11 km ^{2} and 0.14 km ^{2}, respectively. The topography gradually changes from hollow-ridge at the outer ends of the pool-ridge zone to bog forest margin towards the outlets. The total area covered by the sub-catchments of the five outlets was $\sim$ 1km ^{2}, which is $\sim$ 56% of the total bog surface.

The coefficient of determination (R^2) was used as a measure of the strength of the relationship between discharge and catchment size [29]. Average R^2 between discharge from the four outlets and their corresponding catchment sizes were 0.6 in 2008 and 0.4 in 2009 and 2010 (see Fig. 3). Days for which the discharge was strongly correlated with the theoretical catchment size occurred during high flow periods and water tables at or near thebog's surface. A large decrease in R^2 coincided with periods of decreasing discharge and water table depth.

Event dependent contributing area

For each of the selected events, the size of the contributing was calculated based on the outlet's discharge volume (V_Q) over the duration of the event divided by the net precipitation volume ($V_{P_{\text{net}}}$) over the same period (see Materials and Methods - Data analysis). The resulting sizes of the contributing areas are shown in Table 8 and can be compared with the theoretical catchment areas based on the bog's surface gradient.

Event 14 provides a good example of contributing areas that resemble the theoretical catchments based on topography (Fig. 8b). The small storage deficit in autumn with minimal evaporation demands resulted in shallow water tables (see Fig. C.1 for response of water table and discharge to precipitation input per event). This suggests that under wet preconditions the bog's catchments behave according to the common hydrological theory for bogs.

Most events in the summer (events 1 to 4, 7 to 12, and 16 to 18) had smaller contributing areas than the theoretical catchment size. Although some of these events (1 and 4) had larger precipitation input than event 14, which behaved closest to theory, the contributing areas were much smaller. This was caused by lower water tables at the start of the events (Fig. C.1), which would require the available storage to be filled before discharge was generated. A similar situation was observed during events 11, 16 and 18, where the Q5 and Q7 catchments appeared most affected by the dryer preconditions leading to smaller contributing areas.

In contrast, autumn events 5 and 6 and spring event 15 showed much larger contributing areas compared to the theoretical catchments. A reason for this could be that, because of the already high water table, a ponding layer initiated surface runoff. For instance, a large amount of snowmelt water (187 mm) contributed to discharge event 15, corresponding with the largest discharge peak observed during the study period. The contributing areas of Q5 and Q7 doubled during event 5 and 6, but during event15 the contributing areas of Q2 and Q2 were mainly affected. It is plausible that during event 15 the peat surface was still partly frozen, creating frost barriers in places where otherwise overflow points in the ridges between the pools would have occurred, and as a result water was retained in the pool-ridge complex. This could have forced water to flow perpendicular to the ridges towards Q2 and Q3.

Discussion

Transmissivity to control water flow

Based on the paramaters obtained after fitting the relationship between transmissivity and water table depth (Eq. 2), transmissivity was found to change fastest with depth in the pool-ridge zone ($M = 47$, see Fig. 7). The maximum hydraulic conductivity at the peat surface (K_{max}= 47781m d $^{-1}$) obtained from this relationship, too, occurred in the pool-ridge zone. This would correspond to a transmissivity of 1030 m ^{2} d $^{-1}$. To establish connectivity between the pools in the pool-ridge zone, the water level in the pools have to rise to close to the peat surface to benefit from the high transmissivities and allow flow through the ridges. Hollows extending the pool system at the northern and southern ends of the pool complex maintain more constant shallow water tables (comparable to W3), and have a less sharp decrease in transmissivity with depth.

High transmissivities in the upper few cm can be explained by the open structure of the living peat moss, which acts more like vegetation resistance in open water flow than hydraulic conductivity resistance as we know from flow through porous media citepmccarter-ecohydrology-2014. The open structure of living peat moss is mainly due to the lack of decomposition, which decreases the pore diameter and active porosity [28]. Pore diameter and pore geometry determine water storage properties of the peat and control flow of water through the peat [19]. The phenomena of vegetation drag dominated water movement through highly conductive peat is observed in several peatlands [5,25,23] as well as in other wetlands like the Everglades [6]. At low water tables flow resistance in these peatlands was controlled by decreasing pore geometry and active porosity causing increased tortuosity of flow paths. The role of surficial water flow in shallow groundwater systems was also addressed by [22]. For a raised bog with a shallow groundwater table they quantified surface runoff and groundwater flow, revealing the relevance of characteristic horizontal drainage distance that exist at different scales for the hydraulic response of the system.

The observations of variation in water table depth and transmissivity over different ecotopes underline the important role of water table depth in the feedback between discharge and connectivity. To apply the Darcy-Dupuit groundwater model, as proposed by [14], assumptions regarding the homogeneity of flow through the peat matrix have to be made. However, this approximation does not accommodate for the large increase or decrease in transmissivity in response to small changes in water table depth. Nor does it account for spatial variability in transmissivity as a result of different decomposition rates and swelling and shrinking behaviour of microtopographic features. Our field measurements of transmissivity underline the occurrence of this large variability (see Fig. 6). This raises the question whether Ingram's model assumptions are valid for the complex arrangement of pool-ridge systems and hummock and hollow structures found on a raised bog.

Variable contributing catchment size

The contributing area analysis revealed that discharge at outlet Q5 and Q7 was particularly sensitive to initial pool water levels. This indicates that discharge from Q5 and Q7 was strongly driven by the water table depth in the pool-ridge system, causing the pool-ridge system to be either part of the catchment or disconnected. Because transmissivities in large hollows extending the pool system at the northern and southern ends of the bog remained higher, they provided an alternative flow path that came into play when flow along the prevailing slope was interrupted by insufficiently high water levels in the pools. This would explain why, even under base flow conditions, outlets Q2 and Q3 had relatively stable contributing areas, whereas the contributing area of Q5 was more strongly influenced by the water level in the pools. When this occurs water from the pool system flows laterally towards the sides. This is in keeping with previous findings that variation in pool-ridge hydrologic connectivity was a first-order control on runoff response [25]. Furthermore, a study by [10] showed that drainage density can vary by one order of magnitude, suggesting significant differences in connectivity between the expanded and contracted flow networks and their contributing areas.

Although different swelling and shrinking behaviour of microtopographic features can affect the local slope on a bog's surface, the general surface slope of a bog is considered to be stable according to the theories of [17] and [14]. Furthermore, it is assumed that the general surface slope represents the hydraulic gradient. These assumptions led to a rigid interpretation of water distribution on the bog's surface, and inflexible sub-catchment boundaries.

Water table regulated connectivity in pool-ridge zone

If topographic thresholds in the pool-ridge system dictate the hydrologic functioning of the bog, regulating the proportion of active contributing area, this should cause discharge to become most proportional to its theoretical catchment size during wetconditions. To test this hypothesis, we plotted the mean water table depth in the pool system (P7) and mean correlation coefficient between discharge and catchment size of the eighteen events (Fig. 9). Pool system P7 was chosen becauseit is the biggest and most western pool complex in the pool-ridge zone, making it the last threshold connecting the pool-ridge zone and the lower western part of the bog (W2 and W36) to the outlet (Q5). The relationship between discharge and theoretical catchment size was clearly stronger for a water table less than 10 cm below peat surface.

Similar results were obtained by [10], who also found that water table depth was a key factor determining temporal patterns of surface flow connectivity. The stronger coefficient of determination (R^2) between discharge andtheoretical catchment size under wet conditions showed that discharge is only proportional to the theoretical catchment size when connectivity of local storage elements, such as pools and hollows, is obtained. Since the theoretical catchment area of outlet Q5, and part of Q7, include the pool-ridge system, it is likely that the pool-ridge patterning in this part of the bog causes the strong fluctuation in discharge to catchment size correlation. The water table depth plays a crucial role, similarto that of transmissivity, by regulating whether or not a certain amount of precipitation is large enough to raise the water tables to near or at the bog's surface, and this connecting the pools and hollows. If the water table threshold is not reached, parts of the catchment become or remain disconnected.

Conclusion

Beside the limitations in describing peatland development over longer periods, the acrotelm-catotelm conceptâ€™s simplicity is possibly also a limitation for describing the dynamics of patterned bog hydrology over shorter periods. With this study we provide experimental evidence which is consistent with the suggestion that at wet conditions, the flow direction of water changes and is driven by topographical differences. Due to the very high transmissivities at the peat surface, the flow of water at high water table conditions is more like shallow surface flow or channel flow than flow in porous media (i.e Darcy flow). Therefore, small differences in topography can determine the direction of shallow surface flow. Because of this, changes occur inthe shape and size of the contributing areas when a bog changes from dry to wet state. Over 80% of the bog's discharge occurred under non-baseflow conditions with water tables up to 2 cm below the peat surface. In view of the structure of living peat moss (upper 10 cm), with its very high transmissivities (up to 1030 m ^{2} d $^{-1}$), and the shallowness of the water table (less than 5 cm below peat surface) when discharge is generated from the bog's surface, validity of a groundwater flow approach is disputable. Connectivity of local storage elements, such as pools and hollows, possessing large transmissivities when activated, strongly influence the proportionality of the discharge generated from the bog's sub-catchments. This was shown by the strong R^2 between discharge and theoretical catchment size under wet conditions, whereas the R^2 diminished under drier conditions.
Furthermore, we provide further evidence for the need to consider connectivity and storage dynamics of hollow-ridge and pool-ridge systems and their influence on hydrologic behaviour in patterned raised bogs. We believe that the lack of storage and routing processes are an important source of error in current physically based numerical models of patterned raised bog hydrology. Accounting for storage and routing processes is especially important as these influences the travel time of the water and the consequent transport of solutes, such as DOC.

Acknowledgement

We thank EMHI and the staff of Tooma Mire Station for providing data on precipitation, evaporation, and discharge. We would also thank the Endla Nature Reserve for providing accommodation and access to the bog. We are grateful for the discussions with Elve Lode and Edgar Karofeld. We thank Naomi S. Wells for proofreading and English language editing the manuscript.

References

[1] Appels, W.M., P.W. Bogaart, and S.E.A.T.M. van der Zee. Influence of spatial variations of microtopography and infiltration on surface runoff and field scale hydrological connectivity. *Advances in Water Resources*, 34:0 303–313, 2011. doi: 10.1016/j.advwatres.2010.12.003.

[2] Baird, A.J., P.A. Eades, and B.W.J. Surridge. The hydraulic structure of a raised bog and its implications for ecohydrological modelling of bog development. *Ecohydrology*, 10 (4):0 289–298, 2008. doi: 10.1002/eco.33.

[3] Belyea, L.R. and A.J. Baird. Beyond "the limits to peat bog growth": cross-scale feedback in peatland development. *Ecological Monographs*, 760 (3):0 299–322, 2006. doi: 10.1890/0012-9615(2006)076[0299:BTLTPB].

[4] Boelter, D.H. Physical Properties of Peats as Related to Degree of Decomposition. *Soil Science Society of America Journal*, 330 (4):0 606, 1969. ISSN 0361-5995. doi: 10.2136/sssaj1969.03615995003300040033x.

[5] Branham, J.E. and M. Strack. Saturated hydraulic conductivity in Sphagnum-dominated peatlands: do microforms matter? *Hydrological Processes*, 280 (14):0 4352–4362, 2014. doi: 10.1002/hyp.10228.

[6] Choi, J. and J.W. Harvey. Relative significance of microtopography and vegetation as controls on surface water flow on a low-gradient floodplain. *Wetlands*, 340 (1):0 101–115, 2014. doi: 10.1007/s13157-013-0489-7.

[7] Clymo, R.S. The limits to peat bog growth. *Philosophical Transactions of the Royal Society B: Biological Sciences*, 3030 (1117):0 605–654, 1984. doi: 10.1098/rstb.1984.0002.

[8] Darboux, F., P. Davy, C. Gascuel-Odoux, and C. Huang. Evolution of soil surface roughness and flowpath connectivity in overland flow experiments. *Catena*, 460 (2–3):0 125–129, 2002. doi: 10.1016/S0341-8162(01)00162-X.

[9] Eppinga, M.B., P.C. de Ruiter, M.J. Wassen, and M. Rietkerk. Nutrients and Hydrology Indicate the Driving Mechanisms of Peatland Surface Patterning. *The American Naturalist*, 1730 (6):0 803–818, 2009. doi: 10.1086/598487.

[10] Goulsbra, C., M. Evans, and J. Lindsay. Temporary streams in a peatland catchment: pattern, timing, and controls on stream network expansion and contraction. *Earth Surface Processes and Landforms*, 390 (6):0 790–803, 2014. doi: 10.1002/esp.3533.

[11] Grothendieck, G. *nls2: Non-linear regression with brute force*, 2010. R package version 0.1-3.

[12] Holden, J. and T.P. Burt. Hydrological studies on blanket peat: the significance of the acrotelm-catotelm model. *Journal of Ecology*, 910 (1):0 86–102, 2003. doi: 10.1046/j.1365-2745.2003.00748.x.

[13] Ilomets, M., K. Kimmel, C.-G. Sten, and R. Korhonen. *Mires in Estonia and Southern Finland*. GEOGuide Baltoscandia, Tallinn, 2007. ISBN 978–9985–9834–6–1.

[14] Ingram, H.A.P. Soil layers in mires: Function and terminology. *Journal of Soil Science*, 290 (2):0 224–227, 1978. doi: 10.1111/j.1365-2389.1978.tb02053.x.

[15] Ingram, H.A.P. Size and shape in raised mire ecosystems: a geophysical model. *Nature*, 2970 (5864):0 300–303, 1982. doi: 10.1038/297300a0.

[16] Ingram, H.A.P. Hydrology. In Gore, A.J.P., editor, *Mires: Swamp, Bog, Fen and Moor*, volume 4A of *Ecosystems of the world*, pages 67–159. Elsevier, Amsterdam, 1983. ISBN 0-444-42003-7.

[17] Ivanov, K.E. *Water movement in mirelands*. Academic Press Inc., London, 1981. ISBN 0123764602.

[18] Karofeld, E. and H. Tõnisson. Spatio-temporal changes in bog pool bottom topography - temperature effect and its influence on pool development: an example from a raised bog in Estonia. *Hydrological Processes*, 280 (3):0 958–968, 2014. doi: 10.1002/hyp.9624.

[19] McCarter, C.P.R. and J.S. Price. Ecohydrology of Sphagnum moss hummocks: mechanisms of capitula water supply and simulated effects of evaporation. *Ecohydrology*, 70 (1):0 33–44, 2014. doi: 10.1002/eco.1313.
[20] Morris, P.J., J.M. Waddington, B.W. Benscoter, and M.R. Turetsky. Conceptual frameworks in peatland ecohydrology: looking beyond the two-layered (acrotelm-catotelm) model. *Ecohydrology*, 40 (1):0 1–11, 2011. doi: 10.1002/eco.191.
[21] Morris, P.J., A.J. Baird, and L.R. Belyea. The role of hydrological transience in peatland pattern formation. *Earth Surface Dynamics*, 10 (1):0 29–43, 2013. doi: 10.5194/esurf-1-29-2013.
[22] van der Ploeg, M.J., W.M. Appels, D.G. Cirkel, M.R. Oosterwoud, J.-P.M Witte, and S.E.A.T.M. van der Zee. Microtopography as a driving mechanism for ecohydrological processes in shallow groundwater systems. *Vadose Zone Journal*, 110 (3), 2012. doi: 10.2136/vzj2011.0098.
[23] Price, J.S. and D.A. Maloney. Hydrology of patterned bog-fen complex in southeastern Labrador, Canada. *Nordic Hydrology*, 25:0 313–330, 1994.
[24] Price, J.S. and S.M. Schlotzhauer. Importance of shrinkage and compression in determining water storage changes in peat: the case of a mined peatland. *Hydrological Processes*, 130 (16):0 2591–2601, 1999.
10.1002/(SICI)1099-1085(199911)13:16<2591::AID-HYP933>3.0.CO;2-E.
[25] Quinton, W.L. and N.T. Roulet. Spring and summer runoff hydrology of a subarctic patterned wetland. *Arctic and Alpine research*, 300 (3):0 285–294, 1998.
[26] R Development Core Team. *R: A Language and Environment for Statistical Computing*. R Foundation for Statistical Computing, Vienna, Austria, 2008.
[27] Raukas, A. and A. Teedumäe, editors. *Geology and Mineral Resources of Estonia*. Estonian Academy Publishers, Tallinn, 1997. ISBN 9985-50-185-3.
[28] Rezanezhad, F., J.S. Price, W.L. Quinton, B. Lennartz, T. Milojevic, and P. Van Cappellen. Structure of peat soils and implications for water storage, flow and solute transport: A review update for geochemists. *Chemical Geology*, 429:0 75–84, 2016. doi: 10.1016/j.chemgeo.2016.03.010.
[29] Richardson, M., S. Ketcheson, P. Whittington, and J.S. Price. The influences of catchment geomorphology and scale on runoff generation in a northern peatland complex. *Hydrological Processes*, 260 (12):0 1805–1817, 2012. doi: 10.1002/hyp.9322.
[30] Rydin, H., J.K. Jeglum, and A. Hooijer. *The biology of peatlands*. The biology of habitats. Oxford University Press, Oxford ; New York, 2006. ISBN 978-0-19-852872-2 978-0-19-852871-5.
[31] van der Schaaf, S. *Analysis of the hydrology of raised bogs in the Irish Midlands: a case study of Raheenmore Bog and Clara Bog*. PhD thesis, Wageningen University, Wageningen, 1999.
[32] van der Schaaf, S. A single well pumping and recovery test to measure in situ acrotelm transmissivity in raised bogs. *Journal of Hydrology*, 2900 (1-2):0 152–160, 2004. doi: 10.1016/j.jhydrol.2003.12.005.
[33] Spence, C. and M. Woo. Hydrology of subarctic Canadian shield: soil-filled valleys. *Journal of Hydrology*, 2790 (1-4):0 151–166, 2003. doi: 10.1016/S0022-1694(03)00175-6.
[34] Stofberg, S.F, J. van Engelen, J.-Ph.M. Witte, and S.E.A.T.M. van der Zee. Effects of root mat buoyancy and heterogeneity on floating fen hydrology: Effects of Buoyancy and Heterogeneity on Floating Fen Hydrology. *Ecohydrology*, 90 (7):0 1222–1234, 2016. doi: 10.1002/eco.1720.
[35] Tsuboya, T., K. Takagi, H. Takahashi, Y. Kurashige, and N. Tase. Effect of pore structure on redistribution of subsurface water in sarobetsu mire, northern japan. *Journal of Hydrology*, 2520 (1–4):0 100–115, 2001. doi: 10.1016/S0022-1694(01)00448-6.

A. Precipitation and discharge percentiles

Table A.1. Precipitation and discharge percentiles

	90th *P*	75th *P*	50th *P*	25th *P*
P_{net} (mm d^{-1})	12			
Q5 (Ls^{-1})	21	11	5	2
Q7 (Ls^{-1})	15	8	3	1
Q2 (Ls^{-1})	5	2	1	.3
Q3 (Ls^{-1})	6	4	2	1

Table A.2. Flow situations with flow days and amounts

	Days with flow (>0 Ls^{-1})	Total flow (m^3)	
Q5	487	3.6×10^5	
Q7	624	3.3×10^5	
Q2	687	2.2×10^5	
Q3	689	2.7×10^5	
	Low flow (<25th *P*)	Normal flow (>25th – <75th *P*)	High flow (>75th *P*)
Q5	8.3×10^3 (126 d)	1.1×10^5 (248 d)	2.4×10^5 (123 d)
Q7	6.1×10^3 (161 d)	9.0×10^4 (320 d)	2.3×10^5 (157 d)
Q2	2.5 ×	2.0 ×	2.0 ×

	10^3 (172 d)	10^4 (343 d)	10^5 (172 d)
Q3	8.6×10^3 (173 d)	6.2×10^4 (345 d)	2.0×10^5 (173 d)

B. Start and end dates of discharge events

Event 1: 16–6 until 20–6 2008
Event 2: 22–6 until 30–6 2008
Event 3: 6–7 until 21–7 2008
Event 4: 2–8 until 11–8 2008
Event 5: 27–8 until 2–9 2008
Event 6: 26–10 until 10–11 2008
Event 7: 3–6 until 9–6 2009
Event 8: 12–6 until 19–6 2009
Event 9: 12–7 until 19–7 2009
Event 10: 23–7 until 30–7 2009
Event 11: 16–8 until 27–8 2009
Event 12: 28–8 until 3–9 2009
Event 13: 3–10 until 11–10 2009
Event 14: 16–10 until 25–10 2009
Event 15: 20–3 until 27–4 2010
Event 16: 10–6 until 18–6 2010
Event 17: 18–6 until 30–6 2010
Event 18: 1–9 until 11–9 2010

C. Precipitation, discharge and water table of selected events

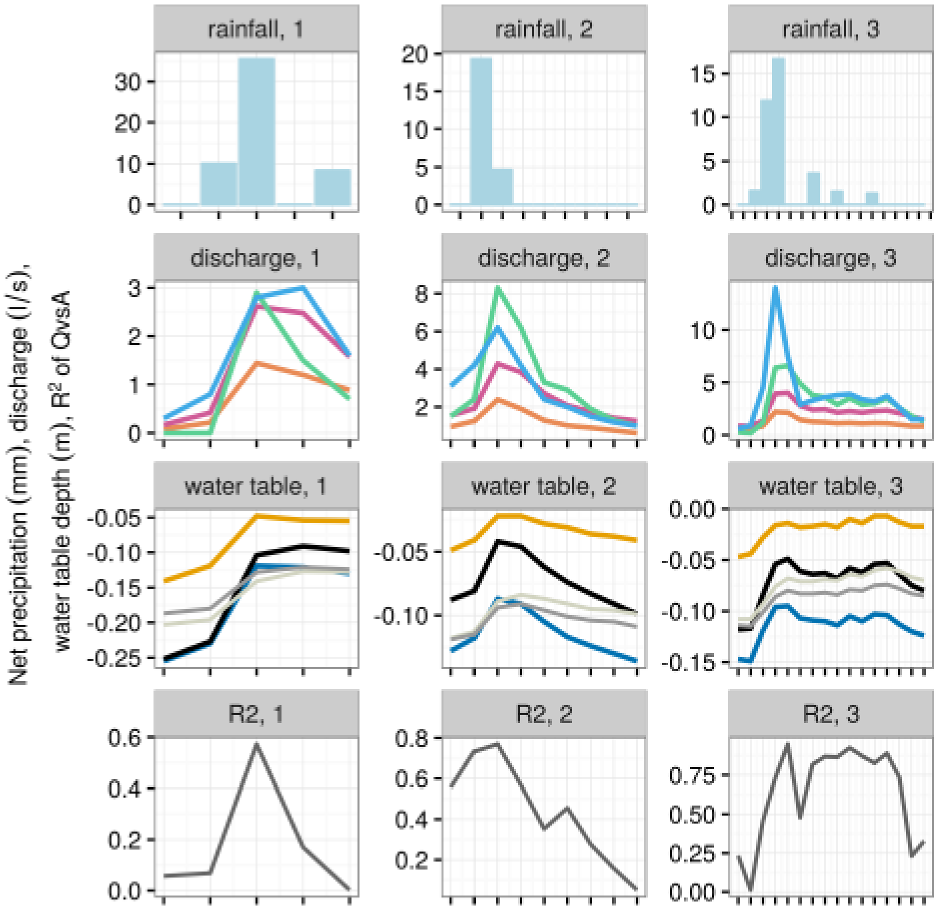

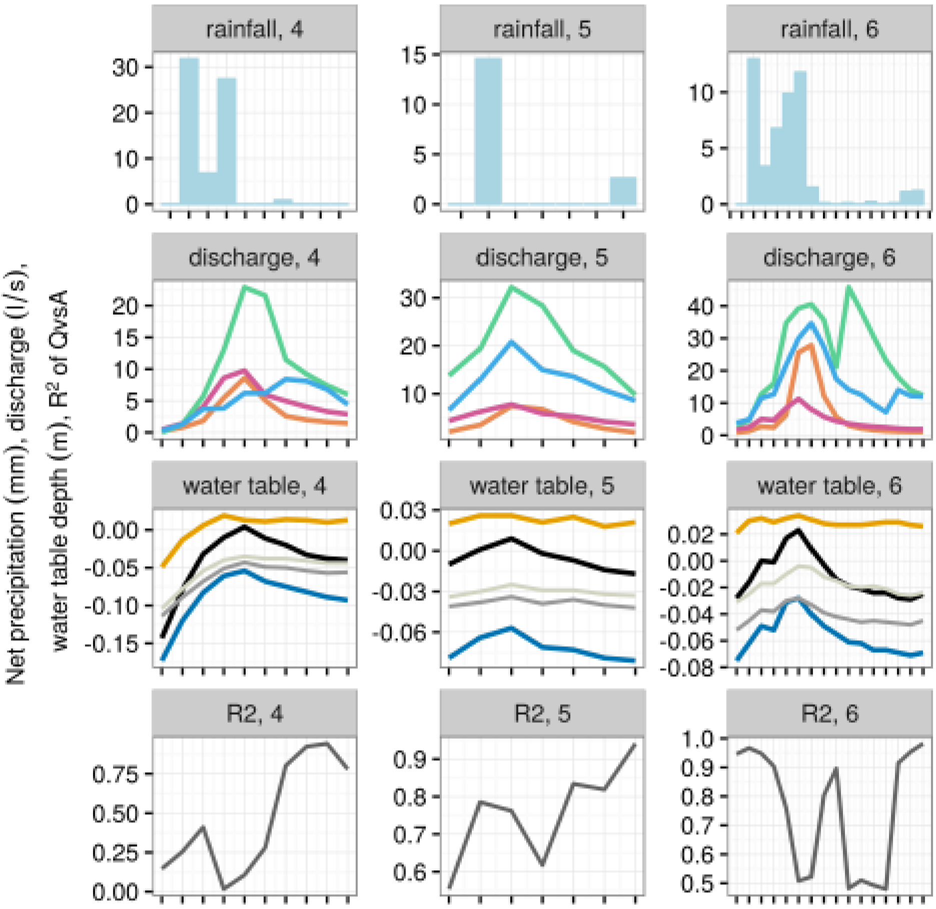
rainfall, 4
rainfall, 5
rainfall, 6
discharge, 4
discharge, 5
discharge, 6
water table, 4
water table, 5
water table, 6
R2, 4
R2, 5
R2, 6
Net precipitation (mm), discharge (l/s),
water table depth (m), R2 of QvsA

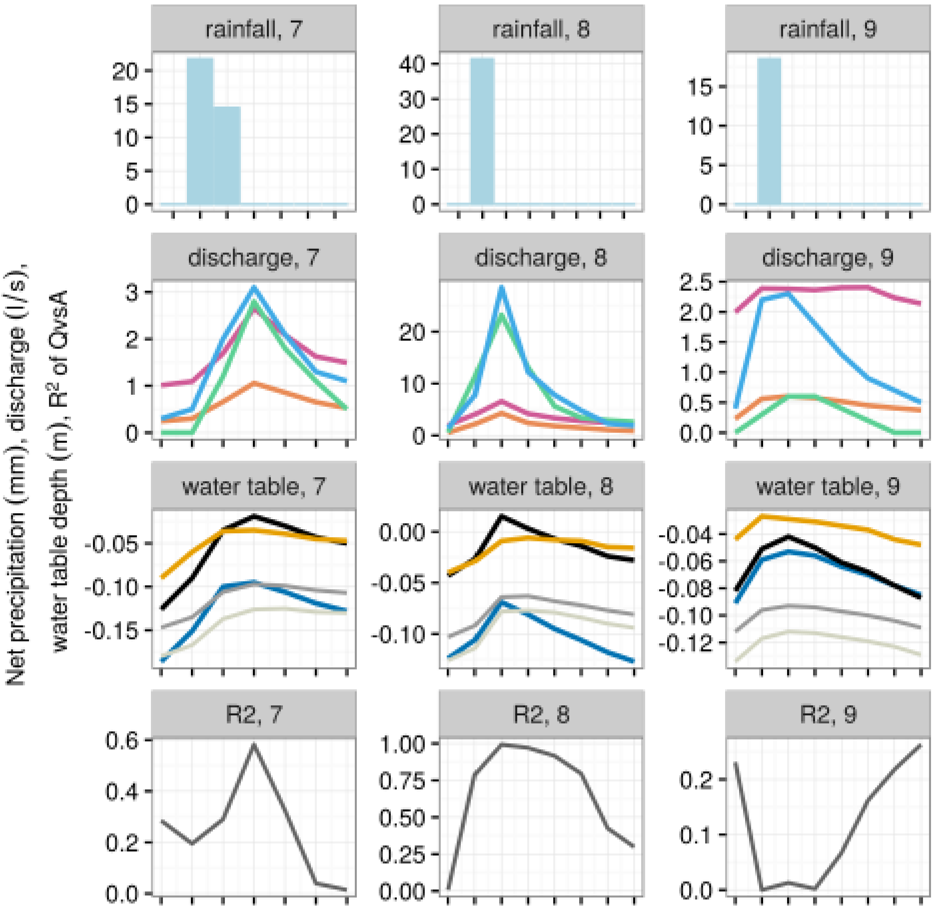
rainfall, 7
rainfall, 8
rainfall, 9
discharge, 7
discharge, 8
discharge, 9
water table, 7
water table, 8
water table, 9
R2, 7
R2, 8
R2, 9
Net precipitation (mm), discharge (l/s), water table depth (m), R2 of QvsA

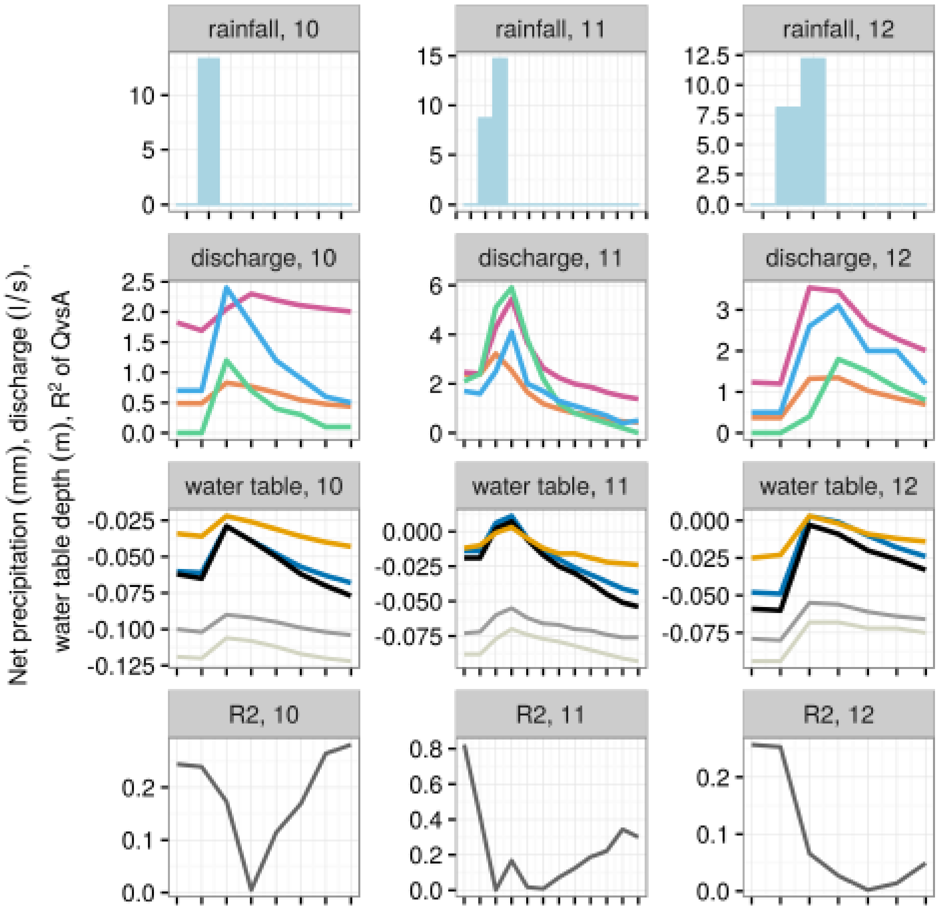

rainfall, 10
rainfall, 11
rainfall, 12
discharge, 10
discharge, 11
discharge, 12
water table, 10
water table, 11
water table, 12
R2, 10
R2, 11
R2, 12
Net precipitation (mm), discharge (l/s), water table depth (m), R² of QvsA

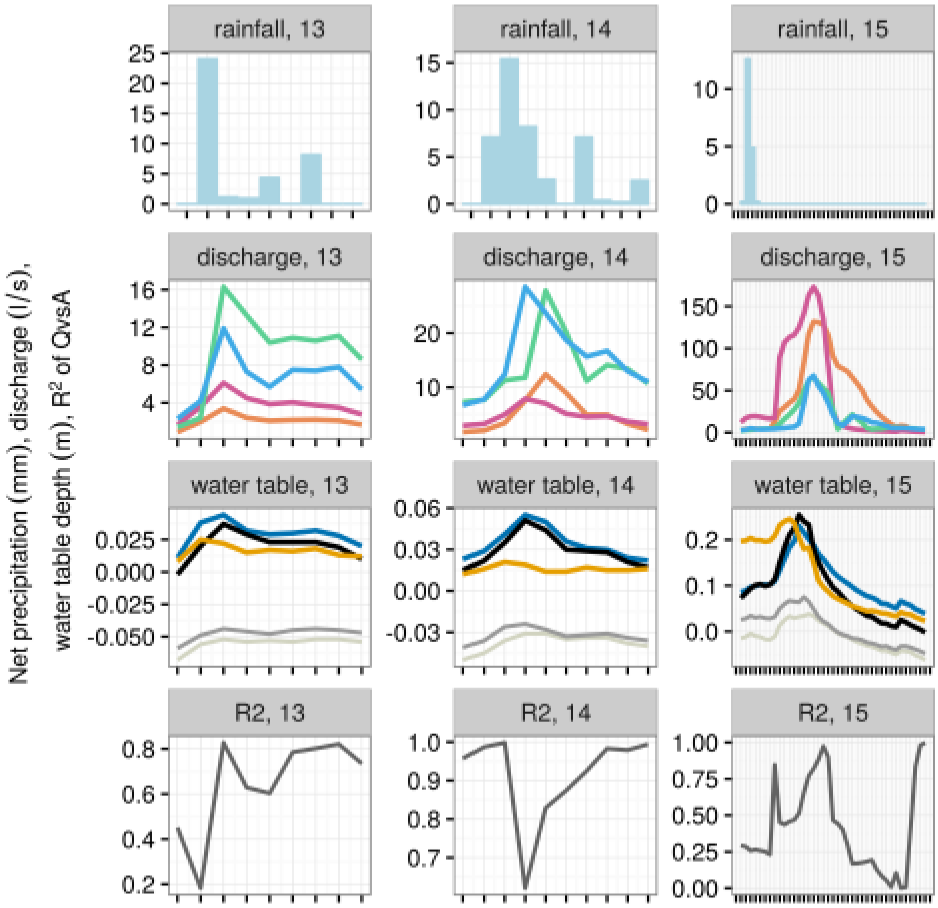
rainfall, 13
rainfall, 14
rainfall, 15
discharge, 13
discharge, 14
discharge, 15
water table, 13
water table, 14
water table, 15
R2, 13
R2, 14
R2, 15
Net precipitation (mm), discharge (l/s), water table depth (m), R² of QvsA

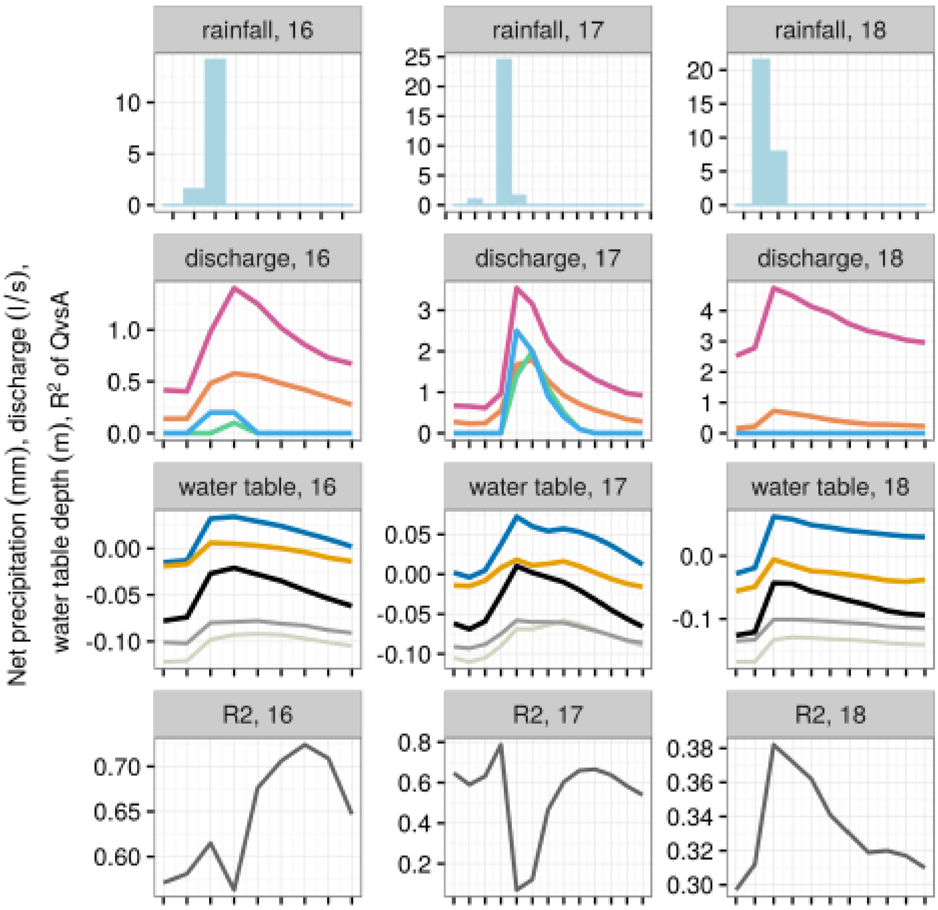

Figure C.1. Individual events (numbered from 1 to 18). Each tick mark on the x-axis represents a day. Note the the y-axes are scaled different. Discharge: blue is Q7, green is Q5, orange is Q2, pink is Q3. Water table depth: black is W2, orange is W3, dark blue is W36. Pool level: light grey is P7, dark grey is P8. R^2, dark grey line, depicts the strength of the correlation between discharge and catchment size.

D. Significant differences between piezometers from Kruskal-Wallis test

detect-weight=true, detect-inline-weight=math

Table D.3. Results (p-values) of the post-hoc Dunn test. Bold values represent piezometers that are not significantly different (p-value: >0.05).

	W36	W2	W37	W3	W4	W31	W38	W5
W2	**0.87**							
W37	$< 2 \times 10^{-16}$	$< 2 \times 10^{-16}$						
W3	$< 2 \times 10^{-16}$	$< 2 \times 10^{-16}$	$< 2 \times 10^{-16}$					
W4	$< 2 \times 10^{-16}$	$< 2 \times 10^{-16}$	$< 2 \times 10^{-16}$	$< 2 \times 10^{-16}$				
W31	$< 2 \times 10^{-16}$	$< 2 \times 10^{-16}$	$< 2 \times 10^{-16}$	$< 2 \times 10^{-16}$	$< 2 \times 10^{-16}$			
W38	1.5×10^{-8}	6.5×10^{-16}	$< 2 \times 10^{-16}$	$< 2 \times 10^{-16}$	2×10^{-4}	$< 2 \times 10^{-16}$		
W5	4.9×10^{-9}	$< 2 \times 10^{-16}$	$< 2 \times 10^{-16}$	$< 2 \times 10^{-16}$	4×10^{-4}	$< 2 \times 10^{-16}$		
W27			$< 2 \times 10^{-16}$	$< 2 \times 10^{-16}$	$< 2 \times 10^{-16}$	$< 2 \times 10^{-16}$	1.8×10^{-12}	4.8×10^{-13}

(a) summer (b) autumn

Figure 1. Summer (a) and autumn (b) 2009 pool system connectivity in the pool-ridge zone of Männikjärve bog. During summer situation pools surface areas are smaller and pool structures more fragmented compared to the wetter autumn situation wherepools have coalesced.

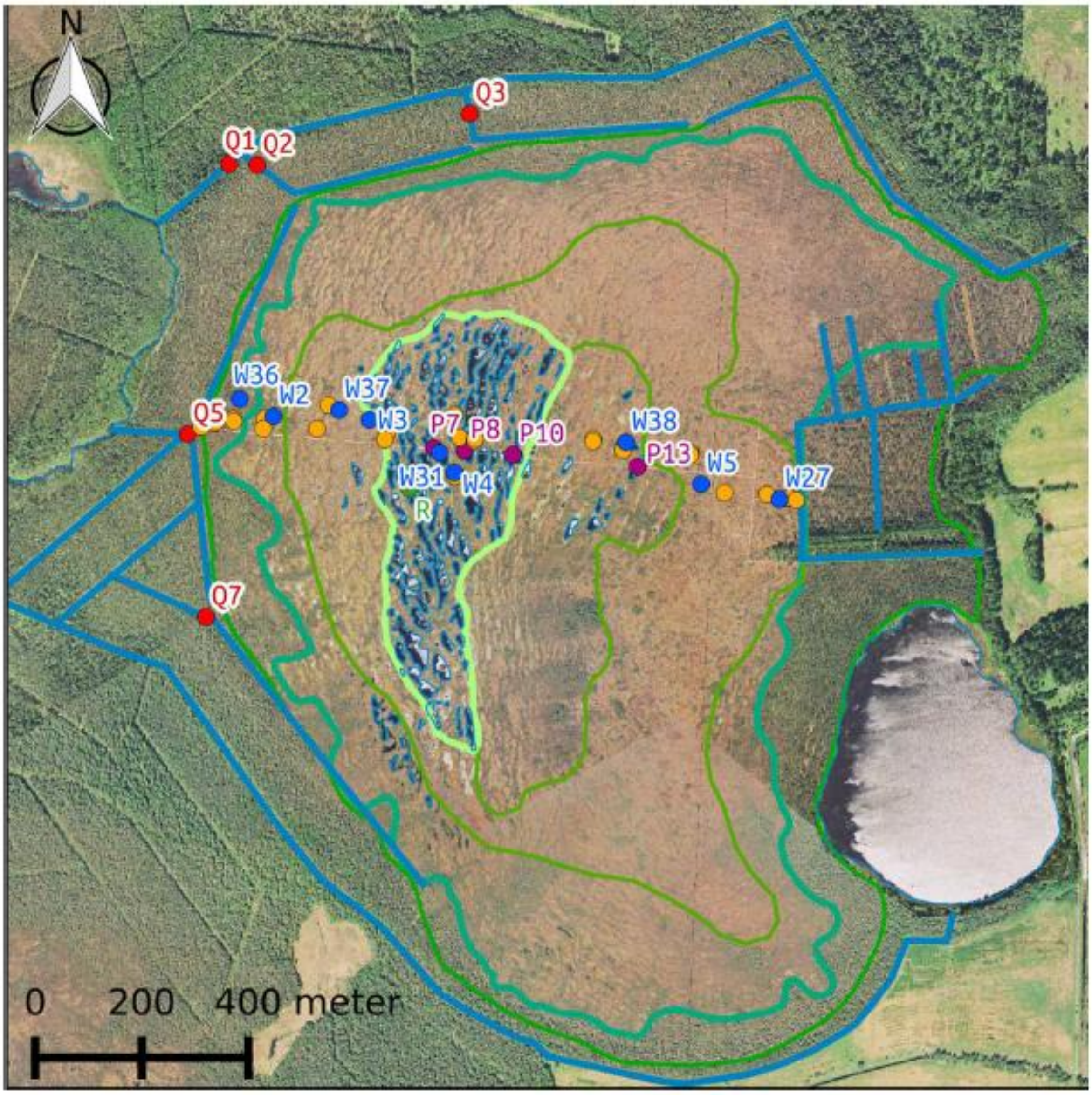

Figure 2. Locations of hydrological instrumentation on Männikjärve bog. Discharge measurement locations (Q) are shown by the red dots, locations of water table (W) and pool water level (P) sites are indicated with blue and purple dots, the locationof the rain gauge (R) is indicated with a green dot, and transmissivity measurement locations are depicted with orange dots. The edge of the bog is indicated by the outer dark green line, the second green line shows the edge of the margin zone, the light green line indicates the border of the pool zone.

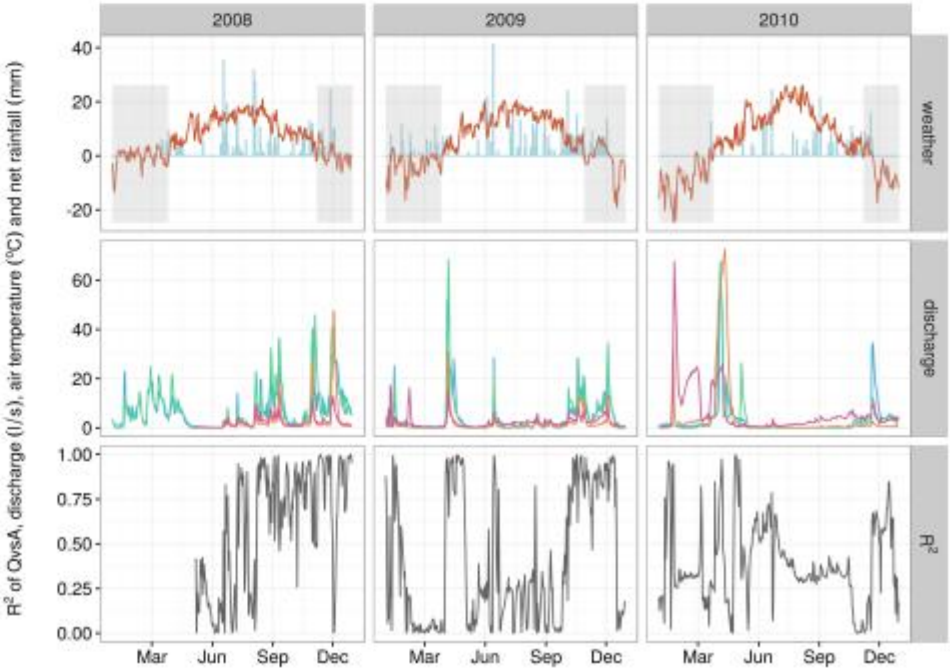

Figure 3. Time series of air temperature (red line), net precipitation (P-ET) (blue bars), discharge, and correlation coefficient (R^2) between discharge and catchment size. The frost free period is shown as the periods without grey shading. Line colours distinguish the different outlets (see Fig. 2 for locations). Discharge: blue is Q7, green is Q5, orange is Q2, pink is Q3. R^2, dark grey line, depicts the strength of the correlation between discharge and catchment size.

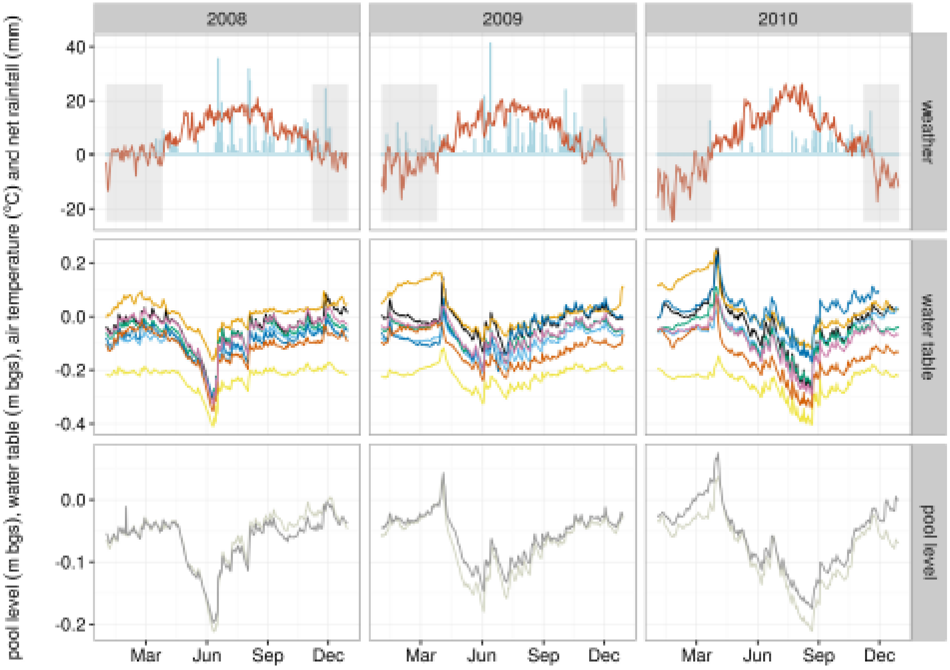

Figure 4. Time series of air temperature (red line), net precipitation (*P-ET*) (blue bars), water table depth and pool level. The frost free period is shown as the periods without grey shading. Line colours distinguish the different wells (see Fig. 2 for locations). Water table depth: black is W2, orange is W3, light blue is W4, dark green is W5, yellow is W31, dark blue is W36, red is W37, purple is W38. Pool level: light grey is P7, dark grey is P8.

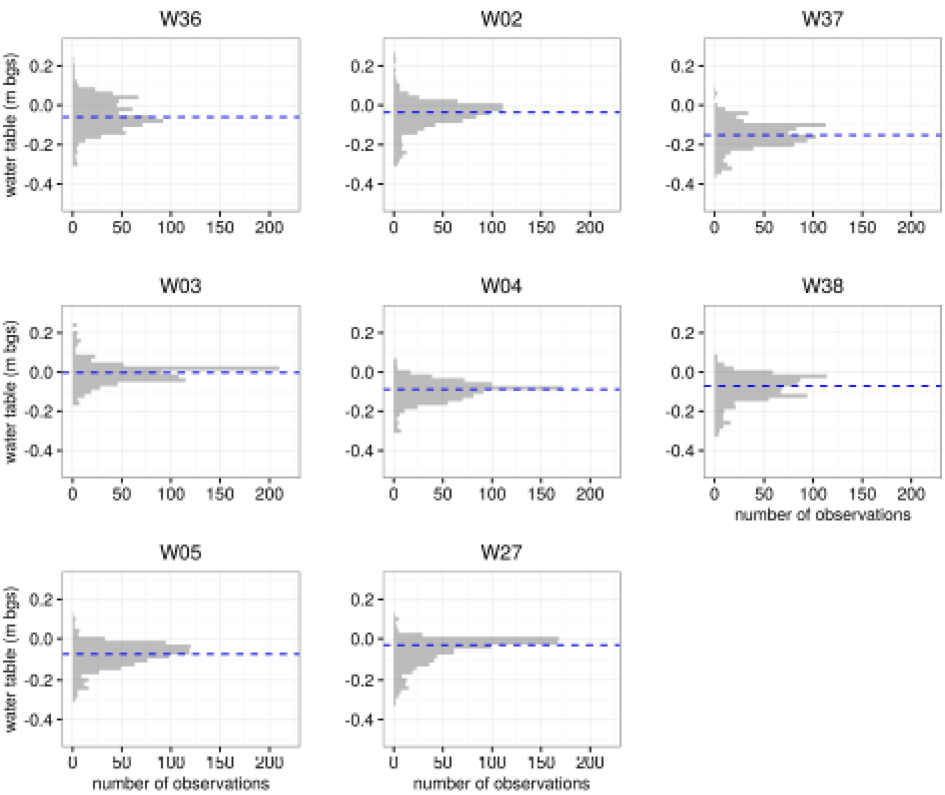

Figure 5. Water table frequency of piezometers from west (upper left) to east (lower right) during 2008-2010. Dotted blue line shows the median.

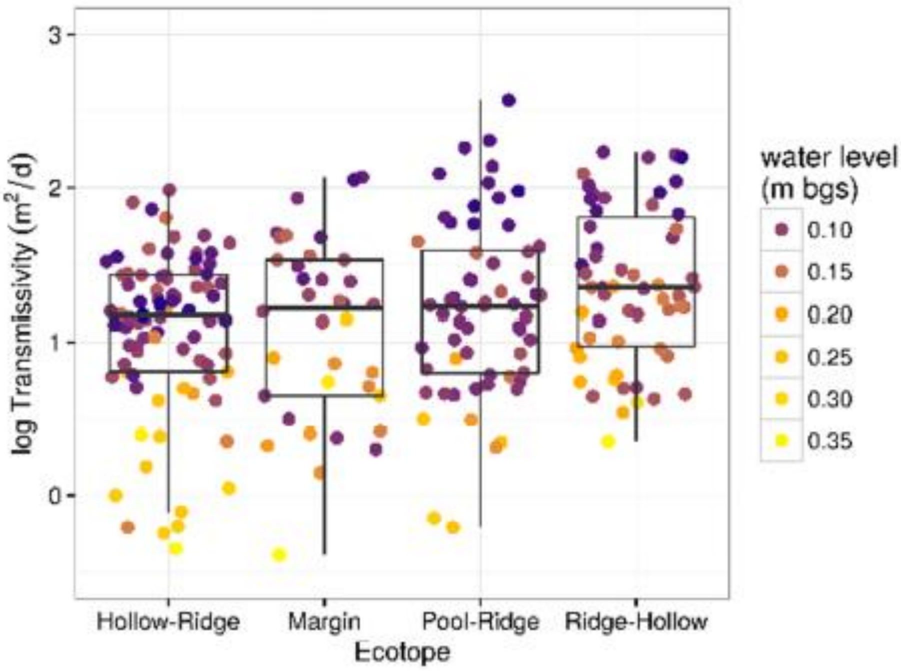

Figure 6. Transmissivity per ecotope zone (number of pits = 9, 5, 5 and 7, in order of appearance). The dots (jittered to prevent over-plotting) depict the individual transmissivity values coloured by the water table at the time of sampling. bgs: below soil surface

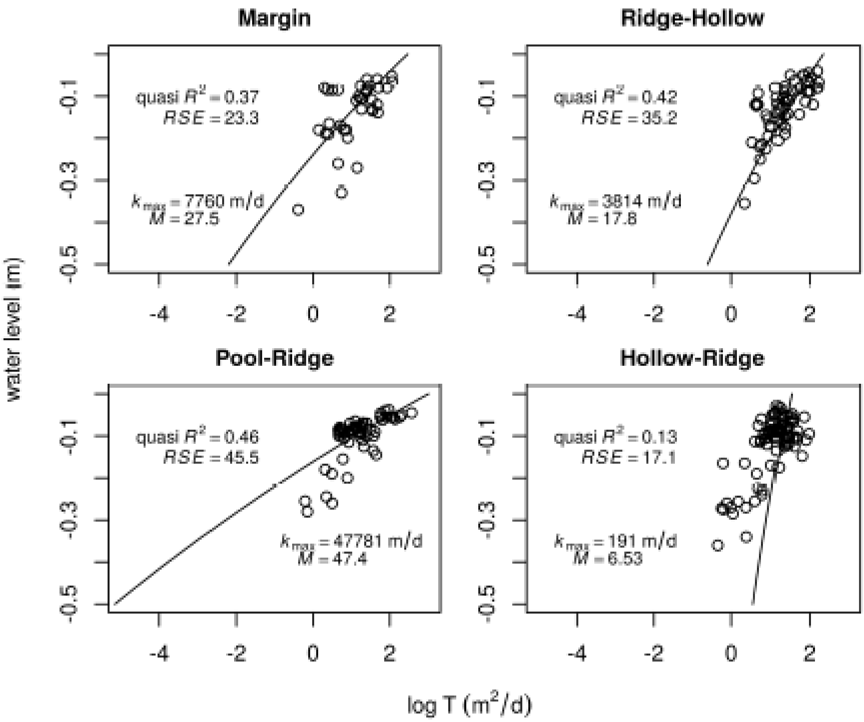

Figure 7. Relationships describing dependency of transmissivity with water table depth according to Eq. 2, fitted to measured transmissivities and water table depths for the four ecotope zones. For each ecotope values for parameters $K_m boxmax$, maximum hydraulic conductivity at the peat surface, and *M*, rate of hydraulic conductivity decrease with depth, are obtained.

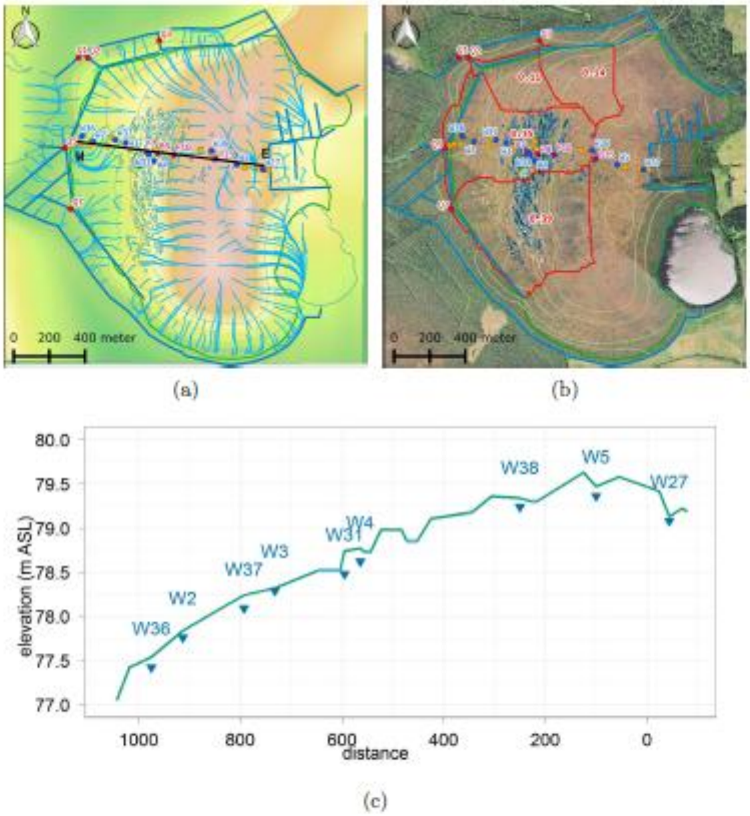

Figure 8. Männikjärve topography. a: DEM and corresponding flowlines (light blue lines) based on slope curves, black line depicts E-W line of sight of cross-section shown in c; b: catchment sizes (km^2) based on multiple flow drainage direction, red lines depict the borders of the (sub)catchments representing the four outlets of the bog; c: bog surface elevation along line of sight E-W, green line depicts the bog surface, light blue lines indicate pool intersects on the cross-section, and blue triangles show the well locations and their mean long-term water table with respect to the bogs surface.

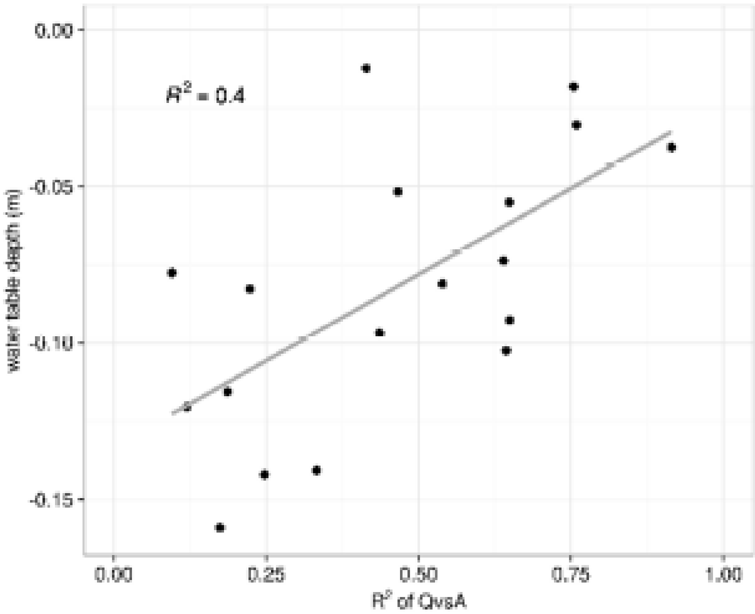

Figure 9. Water table in pool P07 related to catchment size proportionality (R^2). Each dot depicts the mean water table depth and mean R^2 of one of the 18 events.

Table 1. Water balance during frost-free study period at Männikjärve bog. The input of water due to snowmelt is given in "()" as part of the precipitation at the beginning of the frost-free period. Cumulative storage change is shown in "()" as part of the monthly storage balance.

	Precipitation (mm)	Total discharge (mm)	Evapotranspiration (mm)	Storage balance (mm)
2008				
April	32 (32)	20		44 (44)
May	18	2	60	-48 (-4)
June	130	6	127	-8 (-11)
July	89	10	107	-32 (-43)
August	196	35	122	35 (-8)
September	59	36	71	-50 (-57)
October	114	21	51	40 (-18)
2009				
April	13 (90)	51		52 (52)
May	28	2	73	-51 (1)
June	116	13	108	-7 (-6)
July	84	5	71	5 (-1)
August	109	9	124	-27 (-29)
September	53	8	44	0 (-29)
October	118	43	37	38 (9)
2010				
April	33 (178)	132		79 (79)
May	46	8	119	-85 (-7)
June	78	3	91	-20 (-26)
July	75	2	122	-55 (-81)
August	74	4	79	-11 (-92)
September	68	7	36	25 (-68)
October	49	12	10	27 (-41)

Table 2: Contributing areas of different events based on discharge and precipitation volume.

event		Q2	Q3	Q5	Q7	sum
Table 8: continued						
event		Q2	Q3	Q5	Q7	sum
	V_Q (m ^{3})	330	627	441	734	
1	V_{P_net} (m)	0.05				
	A (10 ^{3} m ^{2})	6	12	8	14	40
	V_Q (m ^{3})	961	1797	2488	2229	
2	V_{P_net} (m)	0.02				
	A (10 ^{3} m ^{2})	40	75	104	93	312
	V_Q (m ^{3})	1606	3042	4190	5262	
3	V_{P_net} (m)	0.04				
	A (10 ^{3} m ^{2})	44	83	115	144	386
	V_Q (m ^{3})	2556	3919	8519	4251	
4	V_{P_net} (m)	0.07				
	A (10 ^{3} m ^{2})	38	59	128	64	289
	V_Q (m ^{3})	2483	3241	11949	7638	
5	V_{P_net} (m)	0.02				
	A (10 ^{3} m ^{2})	145	189	697	445	1476
	V_Q (m ^{3})	8332	6008	33722	21228	
6	V_{P_net} (m)	0.05				
	A	170	123	688	433	1413

	(10^3 m^2)					
	V_Q (m^3)	371	1007	639	899	
7	$V_{P_{\text{net}}}$ (m)	0.04				
	A (10^3 m^2)	10	28	18	25	81
	V_Q (m^3)	1262	2384	5409	5754	
8	$V_{P_{\text{net}}}$ (m)	0.04				
	A (10^3 m^2)	31	58	131	139	358
	V_Q (m^3)	321	1582	181	873	
9	$V_{P_{\text{net}}}$ (m)	0.02				
	A (10^3 m^2)	17	86	10	47	160
	V_Q (m^3)	406	1402	242	760	
10	$V_{P_{\text{net}}}$ (m)	0.01				
	A (10^3 m^2)	31	105	18	57	210
	V_Q (m^3)	1496	2724	2134	1598	
11	$V_{P_{\text{net}}}$ (m)	0.02				
	A (10^3 m^2)	64	117	91	68	340
	V_Q (m^3)	516	1414	484	1028	
12	$V_{P_{\text{net}}}$ (m)	0.02				
	A (10^3 m^2)	26	70	24	51	170
	V_Q (m^3)	1634	2915	7344	5141	
13	$V_{P_{\text{net}}}$ (m)	0.04				

	A (10^3 m^2)	42	75	190	133	441
	V_Q (m^3)	4450	4100	1170713323		
14	$V_{P_{\mathrm{net}}}$ (m)	0.04				
	A (10^3 m^2)	102	94	269	306	771
	V_Q (m^3)	13752814083356169495 50				
15	$V_{P_{\mathrm{net}}}$ (m)	0.2				
	A (10^3 m^2)	702	719	287	253	1961
	V_Q (m^3)	295	668	8.6	35	
16	$V_{P_{\mathrm{net}}}$ (m)	0.02				
	A (10^3 m^2)	19	43	1	2	64
	V_Q (m^3)	805	1687	441	510	
17	$V_{P_{\mathrm{net}}}$ (m)	0.03				
	A (10^3 m^2)	30	63	16	19	128
	V_Q (m^3)	358	3346	0	0	
18	$V_{P_{\mathrm{net}}}$ (m)	0.03				
	A (10^3 m^2)	12	114	0	0	126